Continuation of normal modes in finite NLS lattices

Panayotis Panayotaros[†]

[†] Depto. Matemáticas y Mecánica, I.I.M.A.S.-U.N.A.M., Apdo. Postal 20–726, 01000 México D.F., México

June 14, 2010

Abstract

We study the continuation of breather solutions of the discrete NLS equation as the intersite coupling parameter is varied. Considering the case of a finite one-dimensional lattice of N sites, we show the existence of N branches of breathers that persist for arbitrary coupling, thus connecting normal modes of the linear system to breathers of the uncoupled, anticontinuous limit system. The proof is based on global bifurcation theory, applied to the continuation from the weakly nonlinear regime. As the coupling parameter varies these solutions generally change their stability, and we detect parameter regions where trajectories starting near unstable breathers appear to reach equipartition of power.

1 Introduction

In the present work we study some continuation and stability properties of breather solutions of the discrete nonlinear Schrödinger equation (DNLS) in a finite chain. The DNLS equation is a simplified model for physical processes where we see a combination of spatial inhomogeneity and nonlinearity effects. Applications of the DNLS include Bose-Einstein condensates in spatially periodic potentials, see e.g. [AKKS], [LFO], the propagation of laser beams in waveguide arrays and related periodic structures, see e.g. [CLS], and energy transfer in molecular chains, see e.g. [ELS], [KAT]. The DNLS and other nonlinear lattices also pose basic questions on the dynamical foundations of statistical mechanics, see e.g. [ABS].

A breather solution of the DNLS is a time-periodic solution of the form $e^{-i\omega t}A_n$, where ω is the temporal frequency, and A_n is the time-independent breather amplitude at site n. An important feature of breathers is that they are relative equilibria, or equivalently critical points of the energy at hypersurfaces of constant power. Thus the study of breathers is a necessary step for understanding global questions on the dynamics of the DNLS. In [P2] we studied numerically the continuation of breathers as the intersite coupling parameter δ was increased in absolute value. The idea was to use our complete classification of all breathers of the $\delta = 0$ ("anticontinuous limit") and small $|\delta|$ systems and to continue all breathers at once. For a lattice of N sites we saw numerical evidence that there are N breather branches that persist for $|\delta|$ arbitrarily large and converge to the normal modes of the linear limit DNLS. Related numerical results were reported in [BK], [KKC]. In the present work we prove this fact using methods from global bifurcation theory, in particular ideas developed originally in [R]. The global bifurcation results are applied to normal modes of the linear

limit DNLS system. We see that unbounded branches bifurcating from the linear limit system correspond, after rescaling, to breathers that are continued from anticontinuous limit breathers and persist for $|\delta|$ arbitrarily large. The existence of N unbounded disjoint branches follows from the nodal properties of the normal modes of the linear system and some simple observations on DNLS breathers with nodes. The result can be generalized to the DNLS equation with small disorder and other power nonlinearities.

In the second part of the paper we study some questions related to the stability of the breathers that persist for arbitrary δ. As we vary the intersite coupling δ the DNLS system interpolates between the integrable uncoupled system ($\delta = 0$) to the integrable linear system ($|\delta| \to \infty$). The breathers that persist for arbitrary δ are then a simple probe for the changes in the dynamics as we vary δ (near the energies corresponding to these breathers). For $|\delta|$ small the linear stability of breathers can be studied analytically by extrapolating results of [PKF05a], [P1] for breathers of the infinite lattice, and by using some general facts about Hamiltonian matrices, see e.g. [M]. As $|\delta|$ is increased linear stability of the N branches that persist for arbitrary δ is studied numerically. The two branches that consist of global extrema of the energy at fixed power and preserve their lineal stability for all δ and are nonlinearly stable. The remaining $N-2$ branches consist of breathers that change their linear stability as δ is varied and are linearly unstable for some intervals of δ. In the case of linear stability, we can not guarantee nonlinear stability by energy arguments, although we see numerically that trajectories can stay near the breather for long times. In the cases of linear instability we see numerically that trajectories starting near the breather exhibit approximate equipartition of the time average of the power of the different sites. We note that analogous phenomena have been studied extensively for the Fermi-Pasta-Ulam lattice (see e.g. [BP], [FP]), while the DNLS case seems less explored (see [KKFA], [ABS]).

The paper is organized as follows. In section 1 we prove the continuation of N branches of breathers for $|\delta|$ arbitrarily large for the DNLS and some generalizations. In section 2 we examine the stability of these branches numerically. In the case of instability we present and discuss numerical evidence for the equipartition of power.

2 Continuation of breathers in the DNLS equation

We consider the discrete cubic NLS equation

$$\dot{u}_n = i\delta(\Delta u)_n - 2i|u_n|^2 u_n, \tag{2.1}$$

where the index n ranges over the finite set $I_N = \{1, \dots, N\}$ of lattice sites, $u \in \mathbf{C}^N$, and the matrix Δu is defined by

$$(\Delta u)_n = u_{n+1} + u_{n-1} - 2u_n, \quad n = 2, \dots, N-1 \tag{2.2}$$

$$(\Delta u)_1 = u_2 - 2u_1, \quad (\Delta u)_N = u_{N-1} - 2u_N. \tag{2.3}$$

The particular form of $(\Delta u)_1$, $(\Delta u)_N$ is the discrete analogue of *Dirichlet* boundary conditions. The site coupling constant δ is real.

A *breather* solution of (2.1) is a time-periodic solution of (2.1) of the form $u_n = e^{-i\omega t}A_n$, with ω real, and $A = [A_1, \ldots, A_N] \in \mathbf{C}^N$ independent of t. By (2.1), A, ω satisfy

$$-\omega A_n = \delta(\Delta A)_n - 2|A_n|^2 A_n, \quad n \in I_N. \tag{2.4}$$

Note that if A satisfies (2.4) so does $e^{i\phi}A$, for arbitrary real ϕ independent of n. A *real* breather is a breather of the form with $e^{i\phi}\tilde{A}$, where $\tilde{A} \in \mathbf{R}^N$, and $\phi \in \mathbf{R}$ is independent of n. In [P2] it is shown that all solutions of (2.4) with $\delta \neq 0$ are real breathers. We thus restrict our attention to real solutions of (2.4) without loss of generality.

A general problem is to find all solutions of (2.4) as we vary δ. To address this problem we can fix some $C > 0$ and solve the related system

$$-\omega A_n = \delta(\Delta A)_n - 2A_n^3, \quad n \in I_N, \quad \sum_{n=1}^{N} A_n^2 = C. \tag{2.5}$$

Varying δ we expect to obtain families of solutions $(A(\delta; C), \omega(\delta, C))$, moreover we see that the families of solutions of (2.5) obtained for any particular choice of $C > 0$ yield all possible solutions of (2.4). This follows by observing that if $(A, \omega) = (\tilde{A}, \tilde{\omega})$ satisfies (2.4) with $\delta = \tilde{\delta}$, then $A = \tilde{C}^{-\frac{1}{2}}\tilde{A}$, $\omega = \tilde{C}^{-1}\tilde{\omega}$, $\tilde{C} = \sum_{n=1}^{N} \tilde{A}_n^2$, satisfies (2.4) with $\delta = \tilde{C}^{-1}\tilde{\delta}$.

For $\delta = 0$ the solutions of (2.5) are of the form

$$A_n = \pm\sqrt{\frac{\omega}{2}}, \quad \text{for} \quad n \in U_{\pm}; \quad A_n = 0, \quad \text{for} \quad n \in U^c; \quad \omega = \frac{2C}{|U|}, \tag{2.6}$$

where U_+, U_- are disjoint subsets of I_N, $U = U_+ \cup U_-$, $U^c = I_N \setminus U$, and $|U|$ is the cardinality of U. Thus each $\delta = 0$ solution can be labeled by an array of symbols $[s(1), \ldots, s(N)]$, where $s(j)$ is $\pm$ if $j \in U_{\pm}$, and $s(j)$ is 0 if $j \in U^c$. For $|\delta|$ small we have the following general continuation statement, see [P2].

Proposition 2.1 *Fix $C > 0$ and let $(\tilde{A}, \tilde{\omega})$ be a solution of (2.5) with $\delta = 0$. Then there exists a $\delta(\tilde{A}) > 0$, and a unique real analytic one-parameter family of solutions $(A(\delta; \tilde{A}), \omega(\delta; \tilde{A}))$, $|\delta| < \delta(\tilde{A})$, of (2.5) such that $(A(0; \tilde{A}), \omega(0; \tilde{A}) = (\tilde{A}, \tilde{\omega})$. Furthermore, let $\overline{\delta} > 0$ be the minimum of all $\delta(\tilde{A})$ above. Then the set of solutions of (2.5) with $|\delta| < \overline{\delta}$ consists of the solutions $(A(\delta; \tilde{A}), \omega(\delta; \tilde{A}))$ continued from the $\delta = 0$ solutions.*

Thus, for $|\delta|$ sufficiently small, all breathers are continuations of the $\delta = 0$ breathers. Larger values of $|\delta|$ have been studied numerically by several authors, see e.g. [BK], [KK], [P2]. (There are also related works on the DNLS with periodic boundary conditions, see [ELS], [PD], and on the infinite lattice, see [ABK].) In [P2] we see numerically that as δ increases (from $\delta = 0$) breathers undergo bifurcations. In particular we either see fold bifurcations where two (or more) branches collide for some $\delta_0 > 0$ and all breathers disappear for $\delta > \delta_0$, or pitchfork bifurcations where three branches collide at some $\delta_0 > 0$ and only one branch can be continued for $\delta > \delta_0$. For $\delta < 0$ we see a similar picture with signs and inequalities reversed. In addition we see numerically that there are always N branches that can be continued to arbitrary $|\delta|$. We now proceed to state more precisely and prove this fact.

Proposition 2.2 *Fix $C > 0$. There exist N distinct solutions $(\tilde{A}_j, \tilde{\omega}_j)$, $j = 1, \ldots, N$, of (2.5) with $\delta = 0$, and N disjoint continuous one-parameter families $(A(\delta; \tilde{A}_j), \omega(\delta; \tilde{A}_j))$, $\delta \in \mathbf{R}$, of solutions of (2.5) such that $(A(0; \tilde{A}_j), \omega(0; \tilde{A}_j) = (\tilde{A}_j, \tilde{\omega}_j)$, $\forall j = 1, \ldots, N$. As $\delta \to \pm\infty$ each $A_j(\delta, \tilde{A}_j)$, $j = 1, \ldots, N$, converges to a different eigenvector $v^{(j)}$ of Δ. Moreover, the number of sign changes of each breather $A(\delta; \tilde{A}_j)$, $j = 1, \ldots N$, is $j - 1$ and remains constant as δ varies.*

Note that as $|\delta|$ increases in (2.4) we expect intuitively that the linear term dominates so that branches continued to arbitrary δ should converge to solutions of $-\omega A = \delta \Delta A$, i.e. the eigenvectors of the symmetric matrix Δ. The fact that N such branches should exist for all δ is however not immediate. To show it we will use the global bifurcation theory of Rabinowitz [R] on the continuation of linear normal modes, i.e. re-set up the problem as a continuation from the linear limit and then rescale to continue up to the $\delta \to 0$ case.

Note that the eigenvalues $\lambda^{(j)}$, and corresponding eigenvectors $v^{(j)}$ of Δ are

$$\lambda^{(j)} = -2 + 2\cos\frac{j\pi}{N+1}, \quad v_n^{(j)} = \sin\frac{j\pi n}{N+1}, \quad n = 1, \ldots, N; \quad j = 1, \ldots, N. \tag{2.7}$$

$v^{(j)}$ has $j - 1$ sign changes, so that the statement on sign changes in the proposition will follow from the statement that the number of sign changes does not vary along a branch.

To state the global bifurcation theorem, let X with norm $||\cdot||$ be a real Banach space. Let $E = X \times \mathbf{R}$ with the product topology. Consider a function $G : E \to X$ that is compact, continuous, and of the form $G(x, \lambda) = \lambda L x + f(x)$, with L a compact linear operator in X, and $f(x)$ of $o(||x||)$ as $||x|| \to 0$.

The above imply that $G(0, \lambda) = 0$, $\forall \lambda \in \mathbf{R}$. A solution of $G(x, \lambda) = 0$ with $x \neq 0$ is a *nontrivial* solution of $G = 0$. Let $\mathcal{S} \subset \mathcal{E}$ denote the closure in E of the set of nontrivial solutions of $G = 0$. Recall that any $\mu \in \mathbf{R}$ satisfying $v = \mu L v$, with $v \in X$, $v \neq 0$, is a *characteristic value* of L. The *multiplicity* of a characteristic value μ of L is the algebraic multiplicity of the eigenvalue μ^{-1} of L. A *continuum* is a closed, connected set; a *subcontinuum* of a set is a closed, connected subset. We then have the following result of P. Rabinowitz (see [R], Theorem 1.3):

Theorem 2.3 *Let μ be a characteristic value L of odd multiplicity. Then there exists a subcontinuum $\mathcal{C}_\mu$ of $\mathcal{S} \cup \{(0, \mu)\}$ that intersects $(0, \mu)$ and is either (i) unbounded in E, or (ii) intersects some point $(0, \mu')$ with μ' a characteristic value of L, and $\mu' \neq \mu$.*

The condition of odd multiplicity for μ can be also used to show local bifurcation results, although these will not be considered here. Note that scenario (i) includes the possibility of $\mathcal{C}_\mu$ intersecting other points of the form $(0, \tilde{\mu})$, with $\tilde{\mu}$ a characteristic value of L, see e.g. Figure 1. Further regularity conditions on f imply regularity of the continuum of solutions.

We apply Theorem 2.3 to

$$x = \lambda L x + L g(x), \quad x \in \mathbf{R}^N, \quad \lambda \in \mathbf{R} \tag{2.8}$$

$$\text{with} \quad L = (-\Delta)^{-1}, \quad (g(x))_n = -x_n^3, \quad n \in I_N. \tag{2.9}$$

Note that (2.8) is (2.4) with $\omega = \lambda$, $\delta = 1$. The characteristic values of $L = (-\Delta)^{-1}$ are $-\lambda^{(j)}$, $j = 1, \ldots, N$, with the $\lambda^{(j)}$ as in (2.7). They are all simple, and it is immediate that we have the setup of Theorem 2.3 with $X = \mathbf{R}^N$, $f(x) = Lg(x)$. We therefore have:

Lemma 2.4 *Let μ be a characteristic value of $-\Delta$. Then there exists a continuum $\mathcal{C}_\mu$ of solutions of (2.8), (2.9) that intersects $(0,\mu)$ and is either (i) unbounded in $\mathbf{R}^N \times \mathbf{R}$, or (ii) intersects some point $(0,\mu')$ with μ' a characteristic value of $-\Delta$, with $\mu' \neq \mu$.*

We show that the unbounded solution branches of (2.8), (2.9) yield solutions of the breather equation (2.4) with $|\delta|$ arbitrarily small.

Lemma 2.5 *Let $\mathcal{C}_\mu \subset \mathcal{S} \cup \{(0,\mu)\}$ be a continuum of solutions of (2.8), (2.9) that is unbounded in E and intersects $(0,\mu) \in E$, where μ is a characteristic value of $-\Delta$. Then there exists a sequence $\{(x(j),\lambda(j))\}_{j=1}^\infty$ of points of $\mathcal{C}_\mu$ such that $||x(j)||$ diverges as $j \to \infty$.*

Proof. By the definition of $\mathcal{C}_\mu$ there exist sequences $\{(x(j),\lambda(j))\}_{j=1}^\infty$ on $\mathcal{C}_\mu$ for which $||x(j)|| + |\lambda(j)|$ diverges as $j \to \infty$. Suppose that there exists an $M > 0$ such that for all such sequences we have $||x(j)|| \leq M$, $\forall j$. Then, as $j \to \infty$, $|\lambda(j)|$ diverges and $|(x(j))_n| \leq M$, $\forall n \in I_N$. Note that by the definition of $\mathcal{C}_\mu$ we can choose a sequence $\{(x(j),\lambda(j))\}_{j=1}^\infty$ on $\mathcal{C}_\mu$ that diverges in E and satisfies $||x(j)|| \neq 0$, $\forall j$. (Otherwise there exists a ball $\mathcal{B}$ in E such that $\mathcal{C}_\mu$ outside $\mathcal{B}$ is an unbounded subinterval of $\{0\} \times \mathbf{R}$; this would contradict $\mathcal{C}_\mu \subset \mathcal{S}$.) Then, let $B(j) = ||x(j)||^{-1} x(j)$. By (2.4) the $B(j)$ satisfy

$$\lambda(j)(B(j))_n = -(\Delta B(j))_n + 2||x(j)||((B(j))_n)^3, \quad n \in I_N, \quad ||B(j)|| = 1. \tag{2.10}$$

Multiplying both sides by $(B(j))_n$, and summing over $n \in I_N$, the left hand side is $\lambda(j)$ and must diverge as $j \to \infty$, while the right hand side must remain bounded. We thus reach a contradiction. □

Lemma 2.6 *Let $\mathcal{C}_\mu \subset \mathcal{S} \cup \{(0,\mu)\}$ be a continuum of solutions of (2.8), (2.9) that is unbounded in E and intersects $(0,\mu) \in E$, where μ is a characteristic value of $-\Delta$. Then for any $C > 0$ there exists a solution $(\tilde{A}, 0)$ of (2.5) with $\delta = 0$, that can be continued to a solution (A,ω) of (2.5) with δ arbitrarily positive or negative. Moreover, as $A \to \pm A_\mu$ as $\delta \to \pm\infty$, where A_μ satisfies $-\Delta A_\mu = \mu A_\mu$.*

Proof. Consider a notrivial solution $(x,\lambda) \in \mathcal{C}_\mu$ and let

$$\tilde{A} = \pm||x||^{-1} x, \quad \tilde{\omega} = ||x||^{-2}\lambda, \quad \tilde{\delta} = \pm||x||^{-1}. \tag{2.11}$$

By (2.8), (2.9) $\tilde{A}$, $\tilde{\omega}$, $\tilde{\delta}$ satisfy

$$\tilde{\omega}\tilde{A}_n = -\tilde{\delta}(\Delta\tilde{A})_n - 2\tilde{A}_n^3, \quad n \in I_n, \quad ||\tilde{A}|| = 1, \tag{2.12}$$

i.e. (2.5) with $C = 1$, and $\delta = \tilde{\delta}$. By Lemma 2.5 we can choose solutions $(x,\lambda) \in \mathcal{C}_\mu$ with $||x||$ arbitrarily large, i.e. $|\tilde{\delta}|$ can be made arbitrarily small. By Proposition 2.1 these solutions are continuations of solutions of the 2.5 with $\delta = 0$. The statement the follows by varying $||x||$ continuously to make $\tilde{\delta}$ arbitrarily positive or negative. The statement for arbitrary C follows by rescaling. □

Note that for $\{(x(j), \lambda(j))\}_{j=1}^{\infty} \subset \mathcal{C}_\mu$ for which $||x(j)|| + |\lambda(j)|$ diverges as $j \to \infty$ (as in Lemma 2.5), Proposition 2.1, and (2.11) imply that the limit of $||x(j)||^{-2}\lambda(j)$ exists and is nonzero, i.e. the limit is the frequency of a $\delta = 0$ breather.

To complete the proof of Proposition 2.2 we use the fact that $-\omega y_n = \delta(y_{n+1} + y_{n-1} - 2y_n) - 2y_n^3$, $y_n \in \mathbf{R}$, $n \in \mathbf{Z}$, defines an invertible map on the plane, i.e. any pair y_k, y_{k-1} determines the y_n on all other sites. (Solutions of (2.4) correspond to periodic orbits of period at most $2N$ that satisfy y_k for some $k \in \mathbf{Z}$.)

Lemma 2.7 *Let $A \in \mathbf{R}^N$ be a nontrivial solution of (2.5) with $\delta \neq 0$, $C > 0$. Let $m \in I_N$ satisfy $A_m = 0$. Then $m \notin \{1, N\}$ and $A_{m-1} = -A_{m+1}$, with $A_{m-1} \neq 0$.*

Proof. Let A, ω satisfy (2.5), hence (2.4). By (2.4), $A_1 = 0$, or $A_N = 0$ would both imply $A_n = 0$, $\forall n \in I_N$. Similarly $A_k = A_{k-1} = 0$ for k, $k - 1 \in I_n$ implies $A_n = 0$, $\forall n \in I_N$, i.e. A can not vanish in two consecutive sites. Let $A_m = 0$ for some $m \in \{2, \ldots, N-1\}$. Then $A_{m-1} = -A_{m+1}$ is immediate from (2.4), with $A_{m-1} \neq 0$. □

Lemma 2.8 *Let $\mathcal{C}_\mu$ be a continuum of nontrivial solutions of (2.8), (2.9) whose closure intersects $(0, \mu) \in E$, μ a characteristic value of $-\Delta$. Let $\mu' \neq \mu$ be any other characteristic value of $-\Delta$. Then the closure of $\mathcal{C}_\mu$ can not intersect $(0, \mu')$ and is therefore unbounded in E.*

Proof. Assume on the contrary that the closure of $\mathcal{C}_\mu$ intersects $(0, \mu') \in E$, where $\mu' \neq \mu$ is another characteristic value of $-\Delta$. Considering the pairs $(x(s), \lambda(s))$ of $\mathcal{C}_\mu$ we then have that the number of sign changes of x must change along $\mathcal{C}_\mu$. We must then have an $s_0 \in \mathbf{R}$ with $(x(s_0), \lambda(s_0))$ of $\mathcal{C}_\mu$, $x(s_0) \neq 0$, and a $k \in \{2, \ldots, N-1\}$ for which $A = x(s_0) \in X$ satisfies $A_k = 0$, and $A_{k-1}A_{k+1} > 0$. By Lemma 2.7 such an A can not be a nontrivial solution of (2.5) and we have a contradiction. □

Proposition 2.1 on the continuation of the breathers of (2.1) with $\delta = 0$ is easily seen to hold for more general linear intersite couplings, e.g. other finite difference operators for the second derivative. Also we can use more general power nonlinearities of the form $|u_n|^p u_n$, $p \leq 2$, integer, in (2.1). On the other hand our proof of Proposition 2.2 is less general because the node arguments Lemmas 2.7, 2.8 rely on the fact that Δ only couples nearest neighbors. Note that these arguments are analogous to the node arguments used in [R], Theorem 2.3, for nonlinear eigenvalue problems involving second order differential operators on an interval.

In the case of (2.1) with $(\Delta u)_n$ replaced by $(\Delta u)_n + V_n u_n$, $V_n \in \mathbf{R}$, the arguments of Proposition 2.2 go through provided that $\Delta + V$ is (*i*) invertible, (*ii*) has simple eigenvalues, and (*iii*) the eigenvectors of $\Delta + V$ have distinct numbers of sign changes. (By Sturm theory arguments we can see that (*ii*) implies (*iii*).) These assumptions are satisfied when all the $|V_n|$ are sufficiently small, i.e. for small "disorder", and are also easily checked numerically. Note that properties (*i*), (*ii*) can hold in more general situations, e.g. in higher dimensional lattice with disorder where we do not have an analogue of (*iii*). In such cases we can apply Lemma 2.4 but we can not rule out branch collisions.

3 Instabilities of nonlinear normal mode branches

To study the stability of breathers we recall that (2.1) is equivalent to Hamilton's equation

$$\dot{u}_n = -i\frac{\partial H}{\partial u_n^*}, \quad n \in I_N, \quad \text{with} \quad H = \delta\left(\sum_{n=1}^{N-1}|u_{n+1}-u_n|^2 + |u_1|^2 + |u_N|^2\right) + \sum_{n=1}^{N}|u_n|^4. \tag{3.1}$$

An additional conserved quantity of (2.1) is the "power" $P = \sum_{n\in\iota_N}|u_n|^2$.

To study the relative stability of a breather $u = e^{-i\omega t}A$, we write the DNLS in the variables v defined by $u = e^{-i\omega t}v$. (3.1) is then equivalent to

$$\dot{v}_n = -i\frac{\partial H_\omega}{\partial v_n^*}, \quad n \in \mathbf{Z}^d, \quad \text{with} \quad H_\omega = H - \omega P. \tag{3.2}$$

The breather solution $u = e^{-i\omega t}A$ of (2.1) corresponds to a fixed point A of (3.2). Note that we have a circle $e^{i\theta}A$, $\theta \in \mathbf{R}$, of fixed points of (3.2).

Letting $z = [q,p]^T$, with $z_n = [q_n, p_n]^T$, $q_n = \mathrm{Re}v_n$, $p_n = \mathrm{Im}v_n$, $n \in I_N$, Then (3.2) is also written as

$$\dot{z} = J\nabla h_\omega, \quad \text{with} \quad h_\omega = \frac{1}{2}H_\omega, \tag{3.3}$$

and $(Jz)_n = -[p_n, q_n]^T$, i.e. J is the standard symplectic operator. The linearization at a fixed point A of (3.2) is

$$\dot{z} = J\mathcal{H}z, \quad \text{with} \quad \mathcal{H} = \nabla^2 h_\omega(A), \tag{3.4}$$

i.e. $\mathcal{H}$ is the Hessian of h_ω at A (the dependence of $\mathcal{H}$ on ω is suppressed from the notation). Let $\langle f, g\rangle = \sum_{n=1}^N f_n g_n$, with f, $g \in \mathbf{R}^N$, and assume that $A \in \mathbf{R}^N$. Then (3.4) is equivalent to the quadratic Hamiltonian system

$$\dot{z} = J\nabla h, \quad \text{with} \quad h = \frac{1}{2}\langle p, L_+ p\rangle + \frac{1}{2}\langle q, L_- q\rangle, \tag{3.5}$$

where L_+, L_- are $N \times N$ matrices with entries

$$L_+(n,m) = (-\omega + 6A_n^2)\delta_{n,m} - \delta\Delta(n,m), \quad n,m \in I_N, \tag{3.6}$$

$$L_-(n,m) = (-\omega + 2A_n^2)\delta_{n,m} - \delta\Delta(n,m), \quad n,m \in I_N, \tag{3.7}$$

where $\Delta(m,n)$ are the matrix entries of the operator Δ defined by (2.2), (2.3). $L_\pm$, and $\mathcal{H}$ are clearly symmetric.

Consider now a $k-$peak breather solution of (2.4) at $\delta = 0$. By (3.6), (3.7), the spectrum of $\mathcal{H}$ consists of a zero eigenvalue of multiplicity k, an eigenvalue 2ω of multiplicity k, and an eigenvalue $-\omega$ of multiplicity $2(N-k)$. It follows that the spectrum of $J\mathcal{H}$ consists of a zero eigenvalue of multiplicity $2k$, and eigenvalues $\pm i\omega$, each of multiplicity $N-k$. The multiplicity k zero eigenvalue of $\mathcal{H}$ corresponds a multiplicity k zero eigenvalue of L_-.

As the $k-$peak breather $A(0)$ is continued to a breather $A(\delta)$ of (2.4) with $|\delta| \neq 0$, and sufficiently small, by Proposition 2.1, $A(\delta)$ can expanded in a convergent power series in δ. We easily check

that the corresponding expansion of the $L_\pm(\delta)$ are convergent, and their eigenvalues are therefore analytic in δ. Also observe that $L_-(\delta)A(\delta) = 0$, $\forall\delta$. Then the spectrum of $\mathcal{H}$ consists of one zero eigenvalue, $k-1$ eigenvalues of size $O(\delta)$, k eigenvalues $2\omega + O(\delta)$, and $2(N-k)$ eigenvalues $-\omega + O(\delta)$. The zero, and $k-1$ size $O(\delta)$ eigenvalues of $\mathcal{H}$ correspond to eigenvalues of L_-; clearly $\sigma(\mathcal{H}) = \sigma(L_-) \cup \sigma(L_+)$.

The above imply that for $|\delta|$ sufficiently small $\mathcal{H}$ can only be nonnegative or nonpositive for $k = 1$, or $k = N$: for all other k $\mathcal{H}$ has both negative, and positive eigenvalues. Thus nonlinear orbital stability via energy and power conservation is only possible for $k = 1$ or N.

Regarding the spectrum of $J\mathcal{H}$, suppose that for $|\delta|$ sufficiently small the $O(\delta)$ eigenvalues of L_- above are of the form $\rho_1 = 0$, $\rho_2 = c_2\delta^{r_2} + O(\delta^{r_2+1})$, ..., $\rho_k = c_k\delta^{r_k} + O(\delta^{r_k+1})$, with $c_j \neq 0$, r_j positive integers, and $c_j \neq c_{j'}$ if $r_j = r_{j'}$. This *nondegeneracy assumption* implies that the k $O(\delta)$ eigenvalues of $L_-(\delta)$ are distinct for $|\delta| \neq 0$, and small.

Proposition 3.1 *Assume that the k $O(\delta)$ eigenvalues of $L_-(\delta)$ satisfy the nondegeneracy assumption above. Then the spectrum of $J\mathcal{H}$ consists of (i) a double zero eigenvalue, (ii) $2k-2$ eigenvalues of size $O(\sqrt{\delta})$ that can be either real (in pairs $\pm O(\sqrt{\delta})$), or imaginary (in pairs $\pm iO(\sqrt{\delta})$), and (iii) $2(N-k)$ eigenvalues of the form $\pm i(\omega + O(\delta))$. The number of real eigenvalues of part (ii) is the number of negative $O(\delta)$ eigenvalues of L_-.*

Proof. The proof for parts (i), (ii) of $\sigma(J\mathcal{H})$ follows from the arguments used in the infinite lattice, see [P1]. To see the statement on part (iii) of $\sigma(J\mathcal{H})$ we first use the fact that $\lambda \in \sigma(J\mathcal{H})$ if and only if $-\lambda^2 \in \sigma(L_+L_-)$, see [P1], and Gershgorin's theorem, applied to L_+L_-, to see that the remaining $2(N-k)$ eigenvalues of $J\mathcal{H}$ are of the form $\pm i\omega + O(\delta)$. To see that these eigenvalues are on the imaginary axis, let $V_3(\tilde{\delta})$ denote the subspace corresponding to the eigenvalues $\pm i\omega + O(\tilde{\delta})$ of $J\mathcal{H}$ at $\delta = \tilde{\delta}$. Let $h_3(\tilde{\delta})$ denote the quadratic form defined by $\mathcal{H}$, restricted to $V_3(\tilde{\delta})$. By (3.6), (3.7) we have $V_3(0) = \{(q,p) \in \mathbf{R}^{2N} : q_n = p_n = 0, \forall n \in U\}$, and $h_3(0) = -\omega \sum_{n\in U^c}(p_n^2 + q_n^2)$. Thus $h_3(0)$ is negative definite. Suppose that at some $\delta = \delta_1 \neq 0$, $|\delta_1|$ sufficiently small, we have an eigenvalue $\lambda_1 = \pm i\omega + O(\delta_1)$ of $J\mathcal{H}$ that has nonzero real part. Then $h_3(\delta_1)$ must have an equal number of positive and negative squares (see e.g. [M], Lemma 5). This implies that $h_3(0)$ is nondefinite since the number of positive and negative squares of $h_3(\delta)$ is conserved, see e.g. Theorem of p.146 in [M], a contradiction. □

Thus the stability of the breather is determined by the signs of the $O(\delta)$ eigenvalues of L_-. It is possible that the fact that part (ii) of $\sigma(J\mathcal{H})$ belongs to $\mathbf{R} \cup i\mathbf{R}$ can be shown without the nondegeneracy condition. Expansions on the eigenvalues of part (iii) of $\sigma(J\mathcal{H})$ can be also obtained using results from [KKC].

Remark 3.2 *In the infinite one-dimensional lattice $\sigma(J\mathcal{H})$ consists also of three parts. The first two are the same as (i), (ii) here, while the third part consists of two intervals of width $O(\delta)$ that belong to the imaginary axis and are symmetric with respect to the origin, see [P1]. In the numerical computations we see that as we increase the size of the lattice the eigenvalues $\pm i(\omega + O(\delta))$ become denser and "fill" the intervals of the continuous spectrum.*

As $|\delta|$ is increased we see numerically that the linear stability of the breathers that persist for arbitrary $|\delta|$ generally changes. An exception are the breathers that correspond to the global

maxima and minima of the Hamiltonian H on $P = C$. Breather branches can be labeled by their $\delta \to 0$ limit breathers using the notation after (2.6) (some continua of breathers may have more than one $\delta \to 0$ limits, see [P2]). Also, a breather $A = [A_1, \ldots, A_N]$ is *symmetric* if $B = A$, and *antisymmetric* if $B = -A$, where $B = [A_N, \ldots, A_1]$.

In Figure 2 we plot δ versus the real part of the eigenvalues of $J\mathcal{H}$ for the antisymmetric breather $[-1, 1, -1, 0, \ldots]$ of the lattice with $N = 7$. For $\delta \to 0^-$ the breather is linearly stable, but as $|\delta|$ increases we see three intervals of linear instability. As $|\delta| \to \infty$ the breather appears to remain linearly stable. In Figure 3 we plot the same quantities for the antisymmetric breather $[-1, 0, 1, 0, \ldots]$ of a lattice with $N = 7$. (This breather can be written explicitly and is independent of δ.) The breather is linearly stable for $\delta \to 0^-$, and as $|\delta|$ increases we see the appearance of more unstable eigenvalues. As $|\delta| \to \infty$ it appears that the breather remains unstable. The stability picture is similar for larger lattices. In Figure 4 we plot δ versus the real part of the eigenvalues of $J\mathcal{H}$ for the the symmetric breather $[-1, 1, -1, 1, 0, -1, 1, \ldots]$ of a lattice with $N = 13$, with $C = 13$. (In considering larger lattices we make the power proportional to the size of the lattice.) For $\delta \to 0^-$ the breather is linearly stable, and as $|\delta|$ increases we see one interval of instability. As $|\delta| \to \infty$ the breather appears to remain linearly stable, i.e. as in Figure 2. In Figure 5 we consider the symmetric breather $[-1, 0, 1, 0, -1, 0, 1, \ldots]$, with $N = 13$, $C = 13$. The picture is similar to Figure 2, with an increasing number of unstable modes. As $|\delta|$ is increased we expect that the real parts of the eigenvalues of $J\mathcal{H}$ above should remain bounded. This follows by rewriting the DNLS as $u_n' = i(\Delta u)_n - 2i\delta^{-1}|u_n|^2 u_n$, with $' = \frac{d}{d\tau}$, $\tau = \delta t$, i.e. boundedness of the real parts implies that, as expected, the instabilities become slower in the time scale τ as $|\delta|$ is increased and the system becomes linear.

Note that the behavior seen in Figures 2, 4 is exceptional among breathers with given N in that in all other breathers (that are not global maxima or minima of the energy on $P = C$) exhibit a nonmonotonic change in the number of unstable directions is varied, i.e. the typical behavior is that of Figures 2, 4.

We also remark that combining the result of Proposition 3.1 on the number of unstable eigenvalues of $J\mathcal{H}$ with Theorem 3.3 of [KKS] we can see that the $O(\sqrt{\delta})$ imaginary eigenvalues of $J\mathcal{H}$ correspond to positive squares in h, i.e. they have the opposite Krein signature from the $\pm i\omega + O(\delta)$ eigenvalues of $J\mathcal{H}$. Examining the spectra of the breathers of the figures above we see that as δ is decreased all instabilities come from collisions of eigenvalues on the imaginary axis. In fact, the imaginary eigenvalues coming from the origin as δ is decreased from 0 remain away from the origin and we do not have instabilities through passage from the origin. The number of positive and negative squares of h will then remain constant and since instabilities require the collision of imaginary eigenvalues of opposite Krein signature we expect that the number of unstable eigenvalues $n_u(\delta)$ will satisfy $n_u(\delta) \leq 2\min\{n_-, n_+\}$, $\forall \delta < 0$, where $2n_-$, $2n_+$ are the respective numbers of positive and negative squares of h as $\delta \to 0^-$, $\delta \neq 0$. (Similar considerations apply to $\delta > 0$.) For example in Figure 2 we have stability for $\delta \to 0^-$, and $N - k = 1$. Hence $n_- = 1$, and $n_+ = 5$. As δ is decreased we see pairs of eigenvalues $\pm i\omega_2(\delta)$, $\pm i\omega_3(\delta)$ that collide, move off the imaginary axis producing two unstable eigenvalues, return to the imaginary axis, and repeat this pattern two more times, producing the "bubble" patterns of Figure 2. The number of unstable eigenvalues is always ≤ 2. Similarly, in Figure 4 we have $N - k = 2$, and $\min\{n_-, n_+\} = 2$. As δ is decreased we see an initial collision of two pairs of eigenvalues $\pm i\tilde{\omega}_2(\delta)$, $\pm i\tilde{\omega}_3(\delta)$ that yields two unstable eigenvalues and then a complicated pattern where the number of unstable eigenvalues fluctuates between two

and four, until all eigenvalues return to the imaginary axis. The number of unstable eigenvalues is thus always ≤ 4. In Figures 3, 5 we have $N-k=3$, 6, and $\min\{n_-,n_+\}=3$, 6 respectively. As $|\delta|$ is increased we see that the number of unstable eigenvalues increases monotonically up to 6, 12 respectively. This is consistent with successive collisions of pairs of opposite Krein signature.

Remark 3.3 *In [P1] we saw that for $|\delta|$ small we have an approximate diagonalization of h via symplectic transformations that suggests a direct correspondence between the pairs of squares (i.e. positive and negative oscillators and saddles) of h and the eigenvalues of $J\mathcal{H}$. (The resulting numbers of unstable eigenvalues and Krein signatures agree with Theorem 3.3 of [KKS] but the correspondence is not proved.) For larger $|\delta|$ we have less information, i.e. only the number of different types of pairs of squares. Moreover when eigenvalues collide we lose track of the correspondence between eigenvalues of $J\mathcal{H}$ and normal forms of h. It would be desirable to have a more complete picture of this correspondence for large $|\delta|$ as well.*

The dynamical consequences of linear instability also require further study. In what follows we consider the question of "equipartition of power". To define this notion we examine the evolution of the quantities $\overline{p}_n(t)$, $n=1,\ldots,N$, defined by $\overline{p}_n(t)=t^{-1}\int_0^t |u_n(s)|^2 ds$. Assuming that the $\overline{p}_n(t)$ converge to some $\overline{p}_n$ as $t\to\infty$, we have equipartition of power when the $\overline{p}_n$, $n=1,\ldots,N$, are equal. (If the $\overline{p}_n$, $n=1,\ldots,N$, are equal to within a small error, e.g. some $\epsilon>0$, we have approximate equipartition of power, e.g. $\epsilon-$equipartition of power.) In the figures below we plot the average of the $|u_n(t)|^2$ over the discrete times t_j of the numerical integrator's output ($t_{j+1}-t_j$ vary in the range 10^{-3} to 10^{-2}). The reliability of the numerical results and the interpretation of the plotted averages is discussed below, where we also discuss an alternative definition of equipartition.

A first example is shown in Figure 6 where we plot the time t versus the $\overline{p}_n(t)$ for a trajectory that starts near the unstable antisymmetric breather $[-1,0,1,0,\ldots]$ of Figure 3. The system parameters are $N=7$, $C=7$, and $\delta=-1.55$, for which we have four unstable eigenvalues. The time interval shown is $t=40000$. We see that the graphs of the $\overline{p}_n(t)$ roughly overlap, more precisely we see that $\overline{p}_1(t)$, $\overline{p}_N(t)$ converge to 1.03 ± 0.01, while $\overline{p}_2(t),\ldots,\overline{p}_{N-1}(t)$ converge 0.98 ± 0.01. Another example of approximate equipartition is shown in Figure 7 where we plot the $\overline{p}_n(t)$ for a trajectory starting near the symmetric breather $[-1,1,-1,1,0,-1,1,\ldots]$ of Figure 4. The system parameters are $N=13$, $C=13$, and $\delta=-1.5$, for which the breather is unstable. We see that $\overline{p}_1$, $\overline{p}_N$ converge to 0.68 ± 0.01, $\overline{p}_2$, $\overline{p}_{N-2}$ converge to 0.97 ± 0.01, $\overline{p}_3$, $\overline{p}_{N-3}$ converge to 1.05 ± 0.01, while $\overline{p}_4,\ldots,\overline{p}_{N-4}$ converge to 1.08 ± 0.01. In this case the variation of the $\overline{p}_n$ at the edges is more pronounced.

In all the above cases we see that the $|u_n(t)|^2$ fluctuate significantly, i.e. the convergence concerns the time averages. Also we have integrated numerically trajectories starting near some of the linearly stable breathers above. In all such cases, integration over comparable timescales ($t\sim 20000$) shows that the trajectories remain near the breathers and that the $\overline{p}_n(t)$ remain near the initial values of the $|u_n(t)|^2$. Examples are trajectories starting near the breather of Figure 2, at $\delta=-0.82$ where we have linear stability (this value falls within a linear stability window $[-0.895,-0.74]$ between the two larger "bubbles" seen in Figure 2), and trajectories starting near the breather of Figure 5, at $\delta=-0.7$, where the breather is still linearly stable. Note that in both cases the Hessian has both positive and negative eigenvalues. The apparent long time stability may be explained by normal form arguments. There is also the possibility of escape from the vicinity of the breather after a long time.

We note that the Birkhoff ergodic theorem (see e.g. [K], [CFS]) guarantees the convergence of the (exact) time average $\overline{p}_n(t)$ as $t \to \infty$ for almost all initial conditions with respect to the invariant measure $d\mu(C,E)$ on the set $\Sigma(C,E)$ of initial conditions with $P = C$, $H = E$, see e.g. [K], ch. 2, for the construction of $d\mu(C,E)$ in the reduced phase space of [P2]. In fact the convergence here is elementary for all initial conditions since by the regularity of the trajectories and the integrand in $\overline{p}_n(t)$, we have that for $t > M$, M some positive number,

$$\dot{\overline{p}}_n(t) = \frac{d}{dt}\left(\frac{1}{t}\int_0^t |u_n(s)|^2 ds\right) = -\frac{1}{t^2}\int_0^t |u_n(s)|^2 ds + \frac{1}{t}|u_n(t)|^2, \tag{3.8}$$

so that $\sum_{n=1}^N |u_n(t)|^2 = C$, $\forall t \in \mathbf{R}$, implies

$$|\dot{\overline{p}}_n(t)| \leq \frac{1}{t^2}\int_0^t |u_n(s)|^2 ds + \frac{1}{t}|u_n(t)|^2 \leq \frac{2C}{t}. \tag{3.9}$$

Recall that under the ergodic hypothesis (equivalently the hypothesis that $d\mu(C,E)$ is uniquely ergodic) time averages and phase space averages over $\Sigma(C,E)$ are equal, see e.g. [CFS] for precise definitions. While the validity of ergodic hypothesis is not known here, it motivates a second definition of equipartition of power, namely that we have equipartition of power if, $\forall n \in I_N$, the time average $\overline{p}_n$ equals the phase space average of $|u_n|^2$, i.e. the average of $|u_n|^2$ over $\Sigma(C,E)$ with the measure $d\mu(C,E)$. We can also define a notion of approximate equipartition, as for the first definition. In the case of the $N-$site DNLS with periodic boundary conditions, translation symmetry of H, and P implies that the phase space averages of the $|u_n|^2$ are all equal, hence the two notions of equipartition coincide. In the present case it is reasonable to expect that the phase space averages of the $|u_n|^2$ with n away from the boundary become equal as N increases, i.e. we expect that the phase space average definition of equipartition of power should coincide with approximate equipartition in the first definition.

Remark 3.4 *It is expected that for energies near the energy of one-peak breathers the energy hypersurface for $P = C$ is disconnected. In such cases the ergodic hypothesis and (both notions of) equipartition of power fail. Equivalently, equipartition fails due to orbital stability of such localized orbits. Note also that the existence of orbitally stable $N-$peak breathers implies approximate equipartition for nearby initial conditions since the amplitudes at the different sites are close, at least for $|\delta|$ not too large. On the other hand, the orbits corresponding to Figures 6, 7 have different energy ranges and show significant variation in $|u_n(t)|$. Their existence is more likely related to the chaotic behavior seen in [ABS].*

Numerical integrations were performed using a fixed step Runge-Kutta formula of order 4 (RK4), and a variable step integration algorithm (RK78) that chooses the step size so that Runge-Kutta formulas of orders 7 and 8 agree up to a specified tolerance. For small enough step sizes both schemes achieve power and energy conservation to at least 10^{-8} for all trajectories. On the other hand the global error of the numerical integration seems to be strongly dependent on the trajectory. To roughly estimate the time for which numerical and exact trajectories are close we compare numerical trajectories obtained using different step sizes (maximum step sizes for the RK78). For the RK4 we typically use step sizes 10^{-3}, and 0.5×10^{-3}, while for the RK78 we use maximum step sizes 10^{-2}, 0.5×10^{-2}. Halving the step size increases the accuracy of power and energy

conservation and is therefore assumed not to increase roundoff error accumulation. Following the above test, numerical trajectories starting near linearly stable breathers are expected to follow the exact orbits closely, to within 10% for each component, for times up to $t = 30000$ and in some cases longer. In contrast, for trajectories starting near the unstable orbits, different step sizes lead to numerical trajectories that diverge much earlier, at a time of the order of $t = 50$. This is seen for both algorithms, although the divergence is slower for the RK78 scheme. In the two examples of approximate equipartition we presented above we saw a tendency towards approximate equipartition even within these much shorter intervals. For example, in Figure 7 the RK4 scheme is considered reliable for up to about $t = 70$, and we see that the $\overline{p}_n(70)$ are to within 15% of the $\overline{p}_n(40000)$. The RK78 scheme is considered reliable for up to about $t = 120$, by which time the averages are slightly closer to their apparent long time limits. Note that in Figure 6 we have chosen a value of δ that is close to the onset of instability. For larger $|\delta|$ we also see equipartition, however the numerical trajectories obtained with different time steps diverge at even earlier times, when the tendency towards equipartition is less clear. Similar remarks apply to the trajectories starting near the unstable breathers of Figure 5.

The justification for showing the results from longer integrations in Figures 6, 7 is thus twofold. First, we see that the averages reach values close to the long time averages over time intervals for which numerical trajectories are considered reliable. Second, numerical trajectories may shadow exact trajectories so that the time averages are computed accurately and coincide with phase space averages. This scenario is consistent with our observation that while trajectories obtained using different time steps diverge early, their time averages converge to nearby values. On the other hand we can not rule out the possibility that the tendency to equipartition is transient, and that the numerical time averages are far from the exact time averages.

4 Discussion

We have shown the existence of branches of breathers of the DNLS that exist for arbitrary values of the coupling parameter, corroborating earlier numerical results in [P2]. The result applies to the DNLS (and some variants) in a finite one-dimensional lattice and is based on global bifurcation theory and the topological degree. Recently global bifurcation ideas and the equivariant degree were applied to the periodic DNLS in [GA], where however there is less information on the limits of the global branches. In the present case we were able to use some basic observations on the nodes of breathers that do not seem to have analogues in the periodic case. Analogous continuation results for higher dimensional lattices are currently lacking.

We have also used these branches of breathers to probe some aspects of the dynamics of the system in the parameter ranges where coupling and nonlinearity are comparable. We generally see that as the intersite coupling is increased the linear stability of the breathers changes. Some features of these changes can be interpreted theoretically by extrapolating results obtained in the limit of small intersite coupling. We have also seen examples of trajectories that start near linearly unstable breathers and exhibit equipartition of power. Since breathers are critical points of the Hamiltonian on the hypersurface of constant power they are points where the topology of the energy hypersufaces at fixed power can change. It is worthwhile to understand more about the dynamics on the different energy hypersurfaces and the possible qualitative changes as we pass through the

critical energies corresponding to breathers.

Acknowledgments. We would like to thank J. Ize, C. Garcia Azpeitia, and A. Olvera for helpful discussions. This work was partially supported by SEP-Conacyt 50303, and FENOMEC.

References

[ABK] G.L. Alfimov, V.A. Brazhnyi, V.V. Konotop: On classification of intrinsic localized modes for the discrete nonlinear Schrödinger equation, Physica D 194, 127-150 (2004)

[AKKS] G.L. Alfimov, P.G. Kevrekidis, V.V. Konotop, M. Salerno: Wannier function analysis of the nonlinear Schrödinger equation with a periodic potential, Phys. Rev. E 66, 46608 (2002)

[ABS] C. Antonopoulos, T. Bountis, C. Skokos: Chaotic dynamics of N-degree of freedom Hamiltonian systems, Int. J. Bifurc. Chaos 16, 1777-1793 (2006)

[BK] Yu.V. Bludov, V.V. Konotop: Surface modes and breathers in finite arrays of nonlinear waveguides, Phys. Rev. E 76, 046604 (2007)

[BP] D. Bambusi, A. Ponno: On metastability in FPU, Comm. Math. Phys. 264, 539-561 (2006)

[CFS] I.P. Cornfeld, S.V. Fomin, Y.G. Sinai: Ergodic Theory, Springer, New York (1982)

[CLS] D.N. Christodoulides, F. Lederer, Y. Silberberg: Discretizing light behavior in linear and nonlinear lattices, Nature 424, 817-823 (2003)

[ELS] J.C. Eilbeck, P.S. Lomdahl, A.C. Scott: The discrete self-trapping equation, Physica D 16, 318-338 (1985)

[FP] S. Flach, A. Ponno: The Fermi-Pasta-Ulam problem: periodic orbits, normal forms and resonance overlap criteria, Physica D 237, 908-917 (2008)

[GA] C. Garcia Azpeitia: Aplicación de grado ortogonal a la bifurcación en sistémas Hamiltonianos, Doctoral Dissertation, UNAM (2010)

[K] A.I. Khinchin: Mathematical foundations of Statistical Mechanics, Dover, New York (1949)

[KAT] G. Kopidakis, S. Aubry, G.P. Tsironis: Targeted energy transfer through discrete breathers in nonlinear systems, Phys. Rev. Lett. 87, 165501 (2001)

[KK] T. Kapitula, P.G. Kevrekidis: Bose-Einstein condensates in the presence of a magnetic trap and optical lattice: two-mode approximation, Nonlinearity 18, 2491-2512 (2005)

[KKC] T. Kapitula, P.G. Kevrekidis, Z. Chen: Three is a crowd: solitary waves in photorefractive media with three potential wells, SIAM J. Appl. Dyn. Syst. 5, 598-633 (2007)

[KKS] T. Kapitula, P.G. Kevrekidis, B. Sandstede: Counting eigenvalues via the Krein signature in infinite-dimensional Hamiltonian systems, Phys. D 195, 263-282 (2004)

[KKFA] G. Kopidakis, S. Komineas, S. Flach, S. Aubry: Absence of wave packet diffusion in nonlinear systems, Phys. Rev. Lett. 100, 084103 (2008)

[LFO] R. Livi, R. Franzosi, G. Oppo: Self-localization of Bose-Einstein condensates in optical lattices via boundary dissipation, Phys. Rev. Lett. 97, 060401 (2006)

[M] R.S. Mackay: Stability of equilibria of Hamiltonian systems, in R.S. Mackay, J.D. Meiss (Eds.), Hamiltonian Dynamical Systems, p. 137-153, Adam Hilger, Bristol (1987)

[P1] P. Panayotaros: Linear stability of real breathers in the discrete NLS, Phys. Lett. A 373, 957-963 (2009)

[P2] P. Panayotaros: Continuation of breathers in a finite discrete NLS equation, Disc. Cont. Dyn. Syst. B, to appear (2009)

[PD] C.L. Pando, E.J. Doedel: Bifurcation structures and dominant modes near relative equilibria in the one dimensional discrete nonlinear Schrödinger equation, Physica D 238, 687-698 (2009)

[PKF05a] D.E. Pelinovsky, P.G. Kevrekidis, D.J. Frantzeskakis: Stability of discrete solitons in nolinear Schrödinger lattices, Physica D 212, 1-19 (2005)

[R] P.H. Rabinowitz: Some global results for nonlinear eigenvalue problems, J. Functional Analysis 7, 478-513 (1971)

[QX] W. Qin, X. Xiao: Homoclinic orbits and localized solutions in nonlinear Schrödinger lattices, Nonlinearity 20, 2305-2317 (2007)

Figure Captions.

Fig. 1: Examples of bounded and unbounded curves of solutions in $X \times R$.

Fig. 2: δ vs. real part of eigenvalues of $J\mathcal{H}$ for the antisymmetric breather $[-1, 1, -1, 0, \ldots]$, $N = 7$, $C = 7$.

Fig. 3: δ vs. real part of eigenvalues of $J\mathcal{H}$ for the antisymmetric breather $[-1, 0, 1, 0, \ldots]$, $N = 7$, $C = 7$.

Fig. 4: δ vs. real part of eigenvalues of $J\mathcal{H}$ for the symmetric breather $[-1, 1, -1, 1, 0, -1, 1, \ldots]$, $N = 13$, $C = 13$.

Fig. 5: δ vs. real part of eigenvalues of $J\mathcal{H}$ for the symmetric breather $[-1, 0, 1, 0, -1, 0, 1, \ldots]$, $N = 13$, $C = 13$.

Fig. 6: time t vs. $\overline{p}_n(t)$, $n = 1, \ldots, N$, antisymmetric breather $[-1, 0, 1, 0, \ldots]$ (see Figure 2), $N = 7$, $C = 7$, $\delta = -1.55$.

Fig. 7: time t vs. $\overline{p}_n(t)$, $n = 1, \ldots, N$, symmetric breather $[-1, 1, -1, 1, 0, -1, 1, \ldots]$ (see Figure 3), $N = 7$, $C = 7$, $\delta = -1.5$.

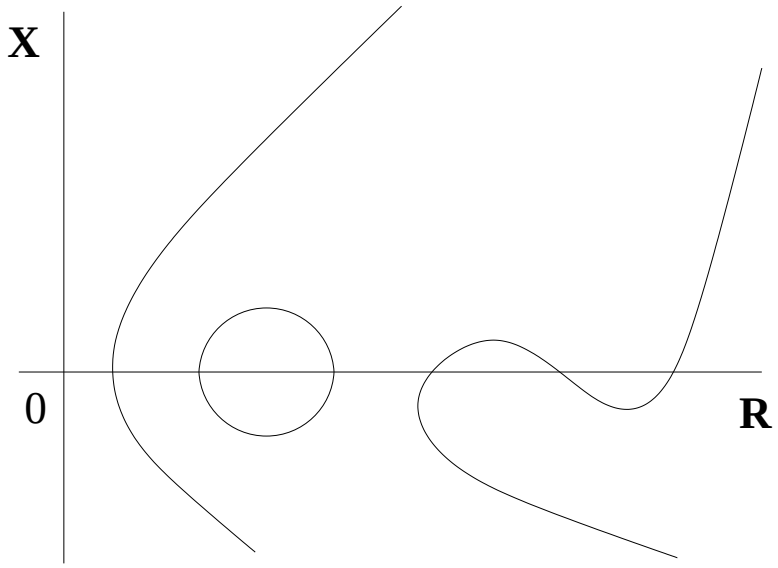

Figure 1

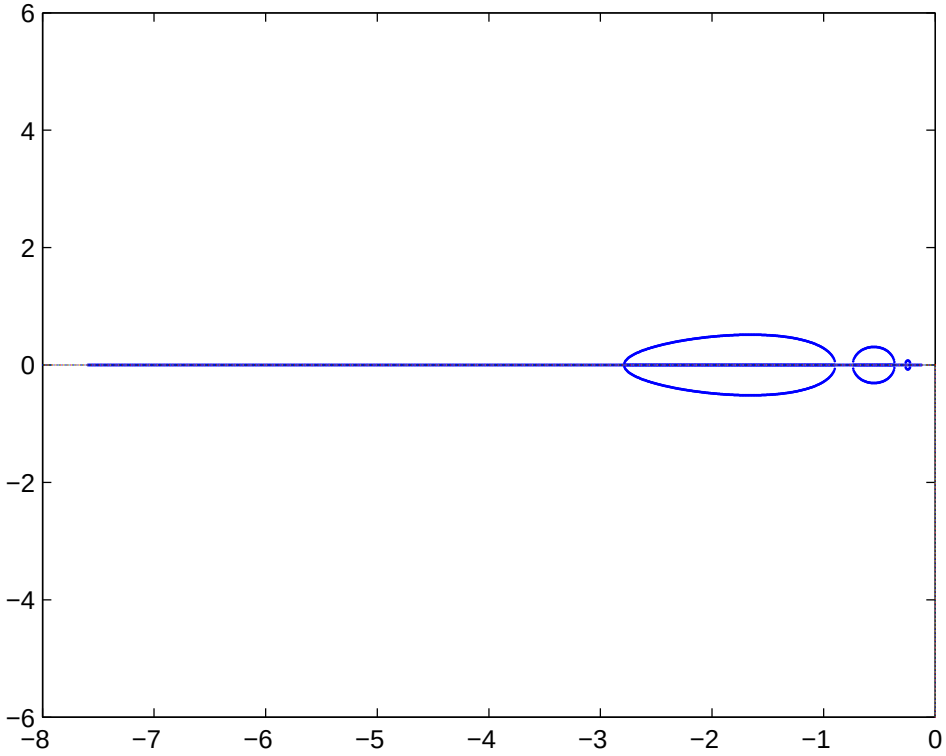

Figure 2

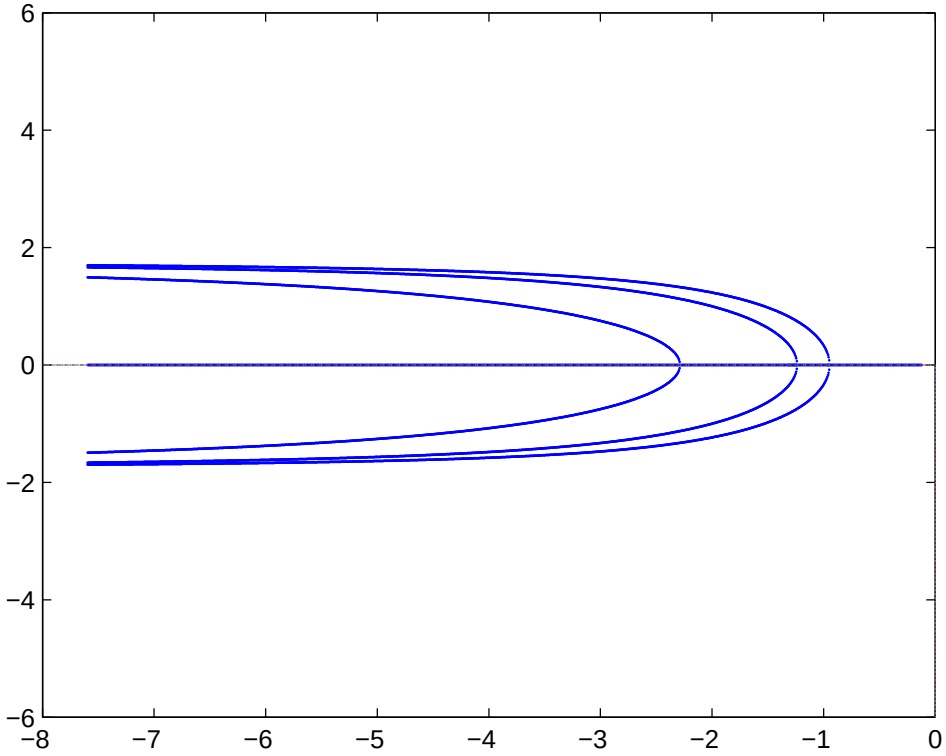

Figure 3

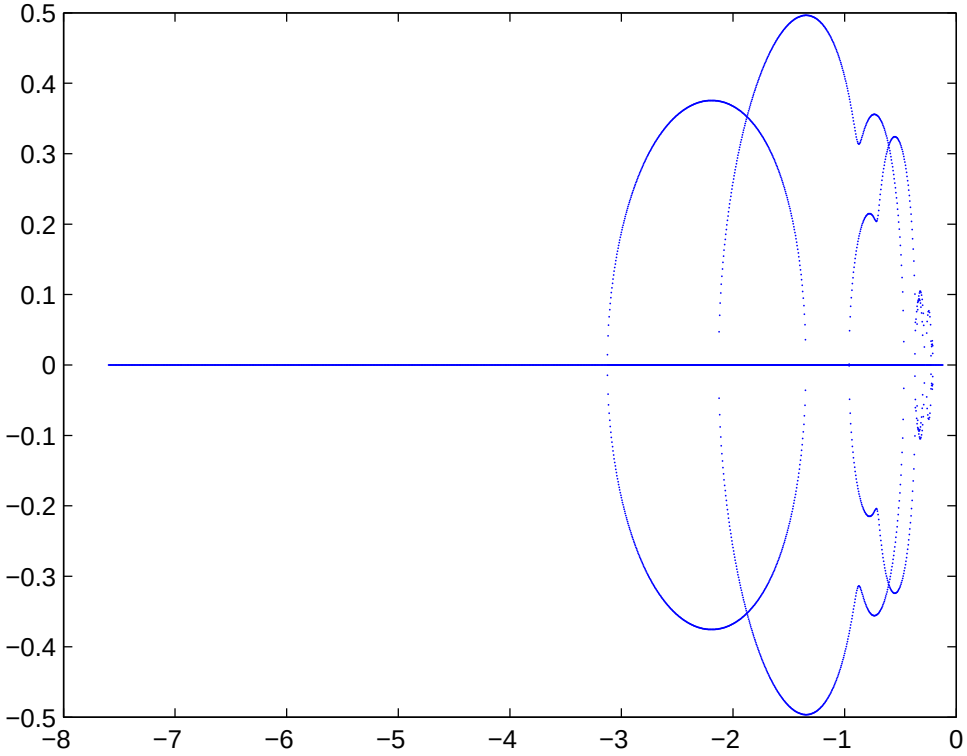

Figure 4

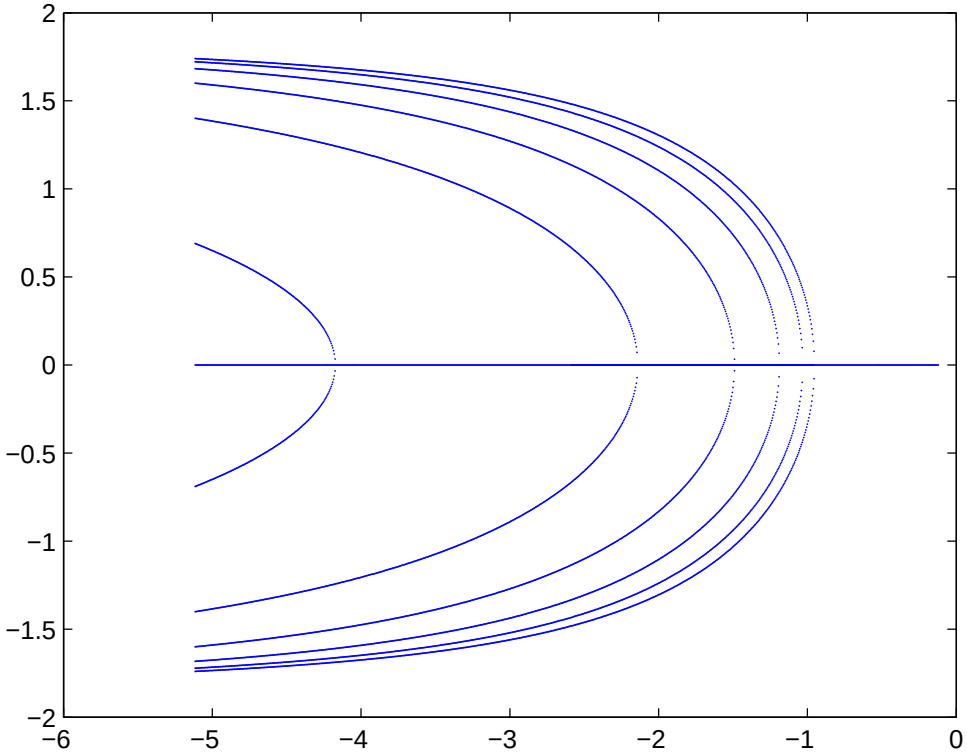

Figure 5

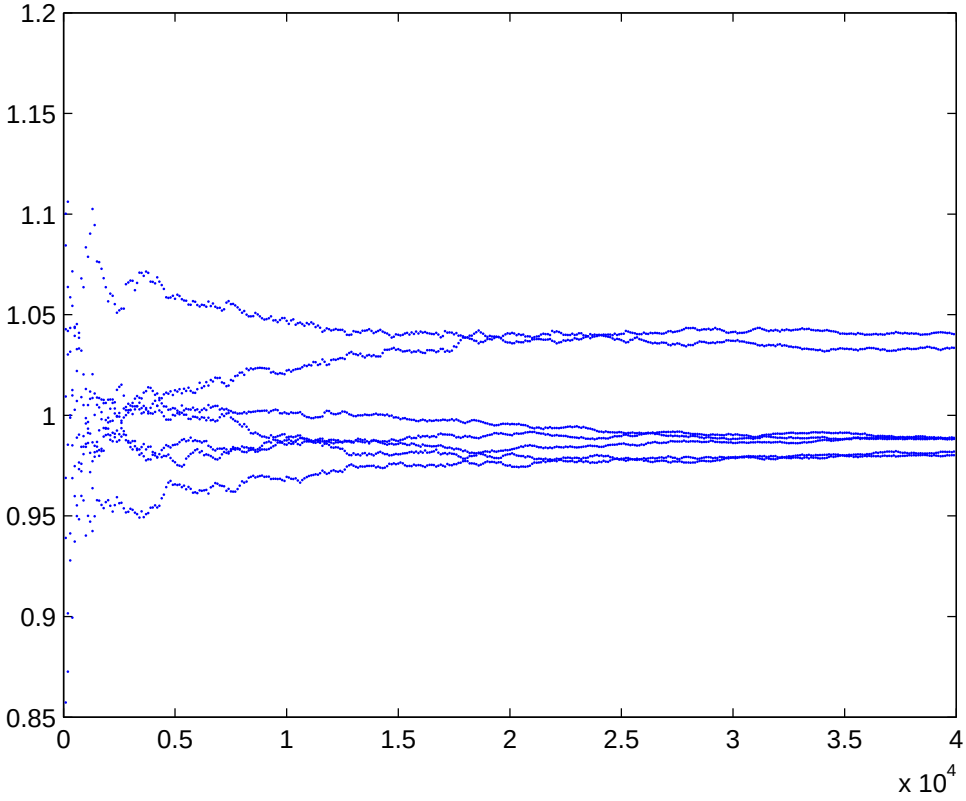

Figure 6

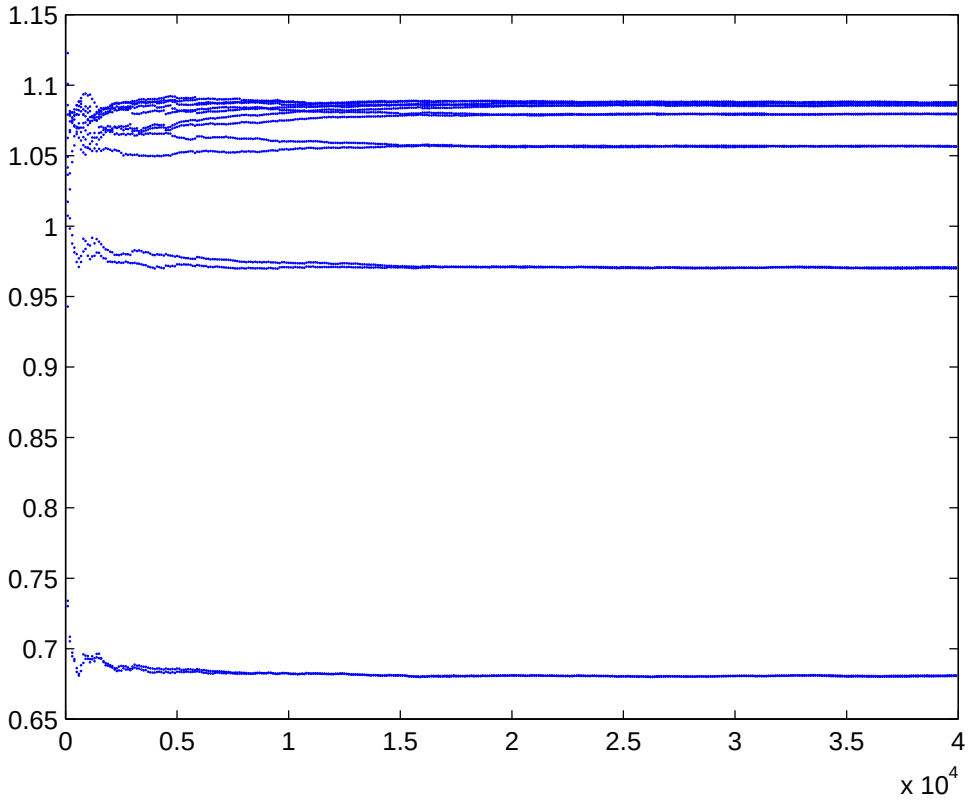

Figure 7